UNIVERSITAT ROVIRA i VIRGILI

Recovery of THF in the process of hydration of Boscalid Technical

Master Thesis in Chemical Engineering

We create chemistry

2024/2025

Student: Valerie Arlenis Sabino Berroa
Company Supervisor: Guifré Aguilò Estopa
University Supervisor: Pere Gabarra

Tarragona

15/05/2025

Acknowledgments

First, and foremost, I would like to thank my family for all the endless support I have received from them. My cats (Kiwi and Miwi), for giving me company while working.

Second, I would like to thank my colleagues at BASF SE. They gave me an opportunity to grow as a professional, not only that, they gave tools that I have extremely valuable in my personal and professional life. From my company tutor, Guifré, from whom I have learned a lot of things, to my co-workers that I shared office (and coffees) with (Gemma, Yasmin, Marta and José). As well as my manager back in my BASF experience, Enrique Pelegrín who wished me the best and gave me the chance to begin my career in the industry.

I'd like to thank the team from Guarantiguetá for all the collaboration with the lab work, they are amazing professionals.

Thanks specially to Pere, for all the trust and patience, understanding how difficult this project has been for me and adapting to my schedules. I also want to thank Frank, for convincing me to pursue this master and for all of his patience as well.

I would also, finally thank my friends for all the unconditional support. My friends from class, that have given me strength to advance in my career, and specially to a friend of mine who is currently fighting the illness she lost her mother to. She is my biggest inspiration.

Thank you so much,

Valerie

Table of contents

Nomenclature

AI	Active ingredient
THF	Tetrahydrofuran
PTS	Powder transfer system
IWM	Iso water moist
y_i	Vapor fraction of component *i* in the mixture
P	Total pressure of the system
x_i	Liquid fraction of component *i* in the mixture
γ_i	Liquid-phase activity coefficient of component *i* in the mixture
P_i^{sat}	Vapor pressure of component *i*
PSD	Pressure swing distillation
ED	Extractive distillation
N_{min}	Minimum number of theorical stages
x_D	Mole fraction of the more volatile component in the distillate
x_B	Mole fraction of the more volatile component in the bottoms
α_{avg}	Average relative volatility of the components
SRK	Soave-Redling-Kwong
PR	Peng-Robinson
PTMEG	Polytetramethylene ether glycol
ED	Extractive distillation
CW	Cooling water
LPS	Low pressure stream
HPS	High pressure stream
TOC	Total operating cost
TAC	Total annual cost
TCI	Total capital investment
DMSO	Dimethyl sulfoxide
EG	Ethylene glycol
TEC	Total energy consumption
R^2	Coefficient of determination
SSE	Sum of squared errors
DFE	Degrees of freedom for error
RMSE	Root mean squared error

1. INTRODUCTION

This project is conducted in collaboration with BASF SE, in the Tarragona site in Spain. More specifically, in the Cluster AP Unit, which is composed by two factories where active ingredients (AI) fungicides and pesticides products are produced in the Kresoxim-metil plant and the Formulation Plant.

The main goal of the project is to determine the viability of recovering one of the raw materials for the Boscalid Iso Water Moist (IWM) production line and its possible applications in the process. To achieve this, simulations and environmental and economical evaluations have been taken to term. The best final option has been optimized and designed via Process Simulation Software.

1.1. Student role in the company

This master's thesis was carried out in collaboration with the same department where I completed both my undergraduate and master's internships. My professional experience was developed within the Process Department of the AP Cluster (Agricultural Products) at BASF SE Tarragona, where I focused primarily on the EHS (Environment, Health, and Safety) area. I worked closely with the deputies responsible for Process Safety, Environmental Protection, and Occupational Safety for the Kresoxim-methyl and Formulation plants.

The main tasks I was involved in included:

Supporting Safety Reviews for both plants: According to company policy, safety reviews are scheduled every 5 or 10 years depending on the hazard level of the facility. Over the course of more than a year, I actively participated in the safety studies carried out at both sites.

Contributing to Occupational Safety activities: Given the extensive portfolio of hazardous chemicals handled at the site, I assisted in various operations related to safety management. In particular, I worked closely with the occupational safety expert in the area of product stewardship, helping track updates in the classification and legislation of substances used in the facilities.

Assisting in incident investigations: I collaborated with Process Department representatives in analyzing incidents related to safety. This experience deepened my understanding of the potential risks associated with chemical production and highlighted BASF SE's strong commitment to safety culture.

Additionally, I had the opportunity to contribute to internal audits, which gave me valuable insight into the rigorous standards and procedures applied within an industrial environment.

1.2. Background

BASF (acronym of *Badische Aniline- und Soda-Fabrik*) is a chemical company that was founded in 1865 in the city of Ludwigshafen, Rhineland-Palatinate by Friedrich Engelhorn with an initial production of dyes.

Currently, BASF holds the first place as the largest chemical company in the world, with approximately 112,00 employees in the organization working in 80 different countries where the group holds operating sites. The company offers a variety of products and services with a wide portfolio of six segments: Chemicals, Materials, Industrial Solutions, Surface Technologies, Nutrition & Care and Agricultural Solutions.

BASF began operations in Spain in 1966 with the creation of BASF Española, headquarters in Barcelona. Over the next decade, it expanded significantly by opening a production center

in Tarragona and acquiring several companies in the paint, leather, and polyurethane sectors. It also established an agricultural experimental station in Seville. The Tarragona site continued to grow with additional facilities for producing plastics and related materials.

The company has strengthened its presence in Spain over the decades through major investments, acquisitions, and consolidation efforts. From 1980 to 2000, it expanded production by becoming the sole owner of the Rubí site, moving operations from Madrid to Guadalajara, and growing the Tarragona facilities with new plants. Key subsidiaries like Curtex and Glasurit were rebranded and fully integrated, and joint ventures such as BASF SONATRACH PropanChem were established.

Between 2001 and 2010, BASF grew through acquisitions of major chemical companies like Engelhard, Degussa, Ciba, and Cognis, leading to the creation of BASF Construction Chemicals and further integration of operations across Spain. By 2009, Spanish activities were managed under the Southern Europe Business Center, and Elastogran became BASF Poliuretanos Iberia. From 2011 to 2019, under the "One Country, One Company" initiative, BASF consolidated all Spanish subsidiaries, launched a new coatings plant in Guadalajara, expanded its agricultural and logistics infrastructure, and acquired Chemetall and Bayer's vegetable seed business (Nunhems Spain). Today, BASF employs over 2,000 people across its various sites in Spain.

1.2.1. Tarragona Site

Located in the largest chemical complex in Southern Europe, BASF Tarragona in La Canonja is one of the main production centers of the company. Spanning over an area of more than 100 hectares, it houses four production plants operated by BASF, a joint venture with SONATRACH, and five plants of third-party companies. The center also has a tank park and a dock at the port of Tarragona.

Figure 1.2.1. Inauguration ceremony of the BASF Tarragona Site on October 30, 1969[1].

[1] BASF. (n.d.). Historia de BASF en España. BASF. Retrieved January 30, 2025, from https://www.basf.com/es/es/who-we-are/BASF-en-Espan-a/Historia

1.2.1.1. BASF Agricultural Solutions

The company's agricultural solutions division is focused in offering customers in the agricultural sector high value products that empower agroproducers to face global challenges such as climate change, an increase in the population and the expansion of developing markets that imply higher food demand.

The company's efforts in the agriculture sector began in 1914 when a research site in Limburgerhof opened to test the production of mineral fertilizers with ammonia synthesis. The Crop Protection market began with the herbicide U46, that launched in the market in 1940. Since then, the company has successfully launched many herbicides, pesticides and fungicides. Nowadays, the company offers many products and solutions such as: Digital Farming, Field Crops Seeds & Traits, Vegetable Seeds, Crop Protection, Public Health, Professional & Specialty Solution and Animal Nutrition.

AP Cluster in Tarragona

The AP (Agricultural Products) Cluster in Tarragona, represents the business division aimed at the agriculture sector. In the site, it two plants, producing both chemical intermediates (raw materials) and final products:

Formulation Plant

The formulations produced in Tarragona are fungicides. The majority of the over 400 different formulations manufactured at this plant are packaged, labeled, and exported to various markets around the world. They are primarily used for crop protection, such as cereals and horticultural crops.

Kresoxim-metil Plant

At the Kresoxim-metil plant, is where the fungicide Active Ingredient that gives name to the plant is produced, along with two other products such m-EOE and Boscalid IWM. These active ingredients serve as raw materials for the production of fungicides and pesticides.

In agrochemicals, active ingredients are the biologically effective components responsible for the product's intended action- such as controlling pests, preventing fungal infections, or promoting plant growth. They are the core substances in products like herbicides, insecticides, and fungicides. These active ingredients are usually combined with other substances (called inert ingredients) to improve application, stability, or overall performance.

Production line of Boscalid ISO Water Moist

Confidential information

During the year 2022, 1.3 million metric tons of THF were consumed all over the globe. 87% of all the produced THF was used as raw material for the PTMEG production. The remaining 13% was utilized as a solvent and other industrial application.

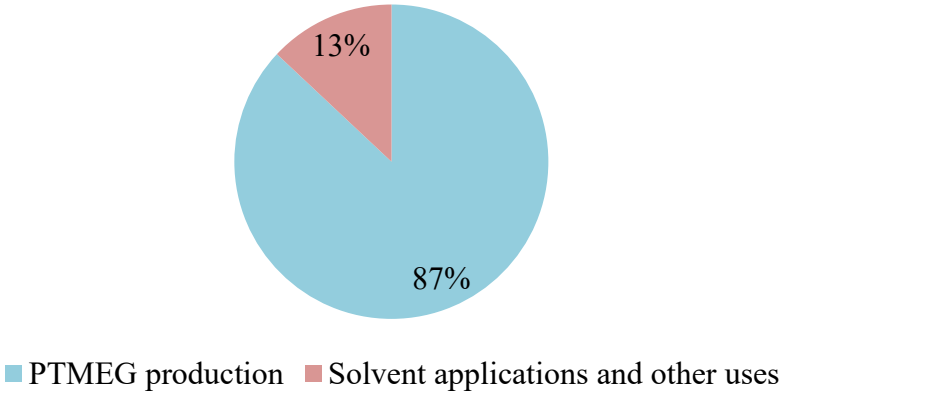

Figure 1.2.1.2 Main applications of Tetrahydrofuran. *(Source: S&P Global Commodity Insights, formerly IHS Markit)*

The geographic location of the main consumers of THF is also related to the current applications in the industry.

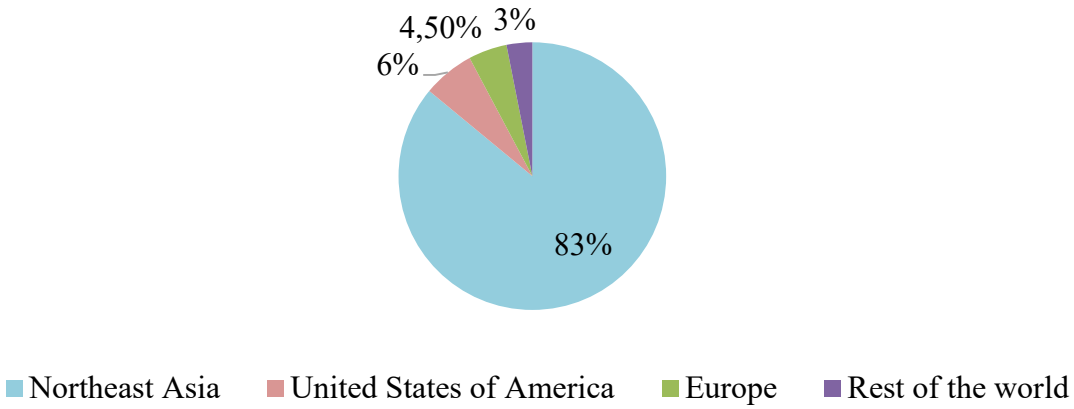

Figure 1.2.1.3 Main global consumers of THF. *(Source: S&P Global Commodity Insights, formerly IHS Markit)*

As can be observed in the chart, in 2022, Northeast Asia accounted for approximately 83% of global THF demand. This is largely due to the region's strong manufacturing base for spandex fibers, polyurethanes, and high-performance elastomers — all of which rely heavily on PTMEG produced from THF. Countries like China, South Korea, and Japan are major producers of textiles, electronics, and automotive components, sectors that use large volumes of these materials.

Sustainability goals and objectives

Chemical industry production processes are highly demanding in terms of energy consumption, which has a direct impact on the increase of local CO_2 emissions in industrialized areas. BASF specializes in providing intermediate products to its customers and is committed to ensuring that the final products that reach consumers have a lower carbon footprint. The strategy to achieve this consists of reducing the CO_2 emissions of production processes.

To reduce its environmental impact, the company has lowered CO_2 emissions from its production processes by approximately 60% since 1990. Looking ahead, BASF has set ambitious climate targets, including:

- A 25% reduction in absolute CO_2 emissions and energy purchases by 2030, compared to 2018 levels.
- Reduce raw materials-related emissions to offer customers a wider range of low carbon footprint products.
- Achieving net-zero greenhouse gas emissions across production, energy, and raw material sourcing by 2050.

Through this approach, the company seeks to achieve climate-neutral production while maintaining a strong commitment to sustainability. This initiative is based on the principles of the circular economy, a model of production and consumption that aims to minimize waste by promoting recycling and the reuse of resources, thus extending the lifecycle and value of materials.

Confidential information

Figure 1.2.1.4 Block diagram of Boscalid IWM Production Line.

Confidential information

1.3. Objectives and scope

The objective of this project is to simulate and design a unit of recovery of THF solvent and water, so both can be reintroduced into the process, evaluating the energy consumption, and environmental impact as well as considering the economic viability of the best alternative of design for the process.

1. Determination of the best technology for the recovery of THF
2. Simulation of the design for the best separation technology
3. Optimization the operating conditions

1.4. Basis of engineering

Confidential information

2. LITERATURE RESEARCH OF AVAILABLE TECHNOLOGIES

In order to achieve a robust design for the recovery of THF and water, various technologies have been evaluated in the alternatives study. This has enabled a rigorous selection of the most suitable separation method for this specific mixture in our process.

The presence of an azeotrope in the mixture implies that, during simple distillation, the vapor and liquid phases can reach identical compositions at a certain point, making further separation by this method unfeasible. As a result, under constant pressure or temperature, the entire mixture can be vaporized or condensed without any change in temperature, pressure, or the composition of the coexisting equilibrium phases.

At low to moderate pressures—common in most industrial applications—the relationship between the liquid and vapor phases at equilibrium can be described as a function of pressure. This correlation accounts for the vapor pressure of each pure component and the activity coefficient of each component "*i"* in the liquid phase.

$$y_i P = x_i \gamma_i P_i^{sat} \quad \text{(Eq.2.1)}$$

Where:
y_i: Vapor fraction of component *i* in the mixture.
P: Total pressure of the system.
x_i: Liquid fraction of component *i* in the mixture.
γ_i: Liquid-phase activity coefficient of component *i* in the mixture.
P_i^{sat}: Vapor pressure of component *i.*

The azeotrope presence can be detected by such a great deviation from Raoult's Law (Eq.2.1) that the equilibrium vapor and liquid compositions become identical.

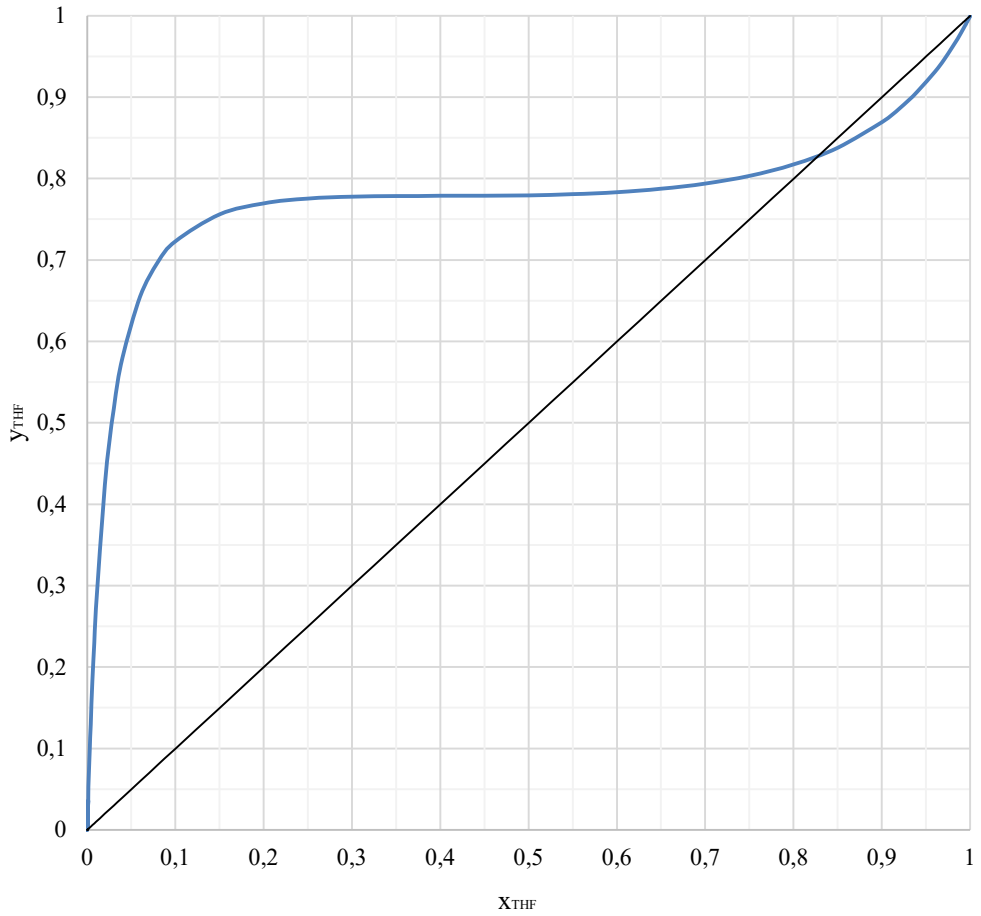

Figure 2.1. Vapor-liquid phase in equilibrium (mixture boiling temperature at atmospheric pressure) for THF/Water mixture.

According to the equilibrium data (Figure 2.1), the azeotrope is located at 83,8 % molar fraction of THF with a boiling temperature of 63,9 ºC at atmospheric pressure.

Table 2.1. Characteristics of the mixture

Substance	**Boiling point (º C)**
THF	66
Water	100
THF/Water (83 %)	64

Due to the liquid phase behavior (THF is completely miscible in water), the azeotrope is considered to be homogenous, and due to the fact that the boiling temperature of the mixture at the azeotrope concentration is lower than the boiling point temperature of both pure components, it is considered to be a positive azeotrope or minimum boiling point azeotrope.

2.1. Separation technologies

When choosing an enhanced distillation method to separate components beyond azeotropic compositions, different approaches can be taken.

1. Choosing an entrainer that gives a residue map curve with specific distillation regions and node temperatures.
2. Exploiting changes in azeotropic composition with total system pressure
3. Exploiting the curvature of distillation region boundaries
4. Choosing an entrainer to cause azeotrope formation in combination with liquid-liquid immiscibility

Depending on these different approaches, the following technology options are available in the industry to achieve the desired separation.

Table 2.1.1. Technology alternatives for separation of azeotropic mixtures

Technology	**Feasible**	**Reasoning**
Vacuum Distillation	Yes	Compatible for Process
Pressure Swing Distillation	No	Operation pressures out of range
Salt distillation	No	Risk of affecting quality in the process
Reactive distillation	No	Risk of affecting quality in the process
Extractive distillation	Yes	Compatible for process
Azeotropic distillation	No	Energy intensive
Membrane Separation	No	Incompatible solid phase in the feed (fouling in the membrane will lead to malfunctioning)
Adsorption	No	High cost of adsorption material and regeneration
Azeotropic Crystallization	No	High energy cost for mixture cooling until crystallization
Flash evaporation	No	Risk for Process Safety

In the following sections (2.1.1 and 2.1.2), the two feasible design alternatives are examined in more depth.

2.1.1. Extractive Distillation

Extractive distillation is a partial vaporization process that involves adding a miscible, highly boiling, nonvolatile separation agent—commonly referred to as a solvent—to an azeotropic or non-azeotropic feed mixture. The purpose is to modify the relative volatilities of the key components without forming any new azeotropes.

This technique is typically used to separate mixtures with close boiling points, azeotropes, or systems with pinched distillation curves, where conventional single-feed distillation is either economically unfeasible or technically impractical. It also enables the recovery of products located at saddle points in the residue curve map—something not usually achievable through standard distillation methods.

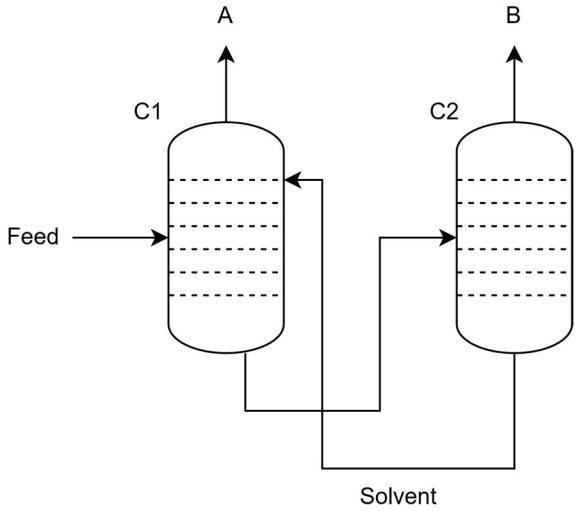

Figure 2.1.1. Extractive distillation schematics.

The classical configuration of an extractive distillation process for separating a binary mixture typically involves two columns: an extractive distillation column (C1) and a solvent recovery column (C2). This setup is especially useful for mixtures with components that exhibit low relative volatility or form a minimum-boiling azeotrope, where conventional distillation is ineffective.

In column C1, the solvent—selected for its high boiling point and low volatility—is introduced at a high concentration a few stages below the condenser but above the main feed stage. This strategic placement ensures that the solvent remains primarily in the liquid phase throughout the lower section of the column, enhancing the relative volatility difference between the key components.

Component A, which is less strongly associated with the solvent, is separated at the top of C1 as an almost pure distillate. Since the solvent is nonvolatile, only a limited number of rectifying stages above the solvent feed point are required to prevent solvent entrainment in the overhead product.

The bottom product from C1, composed mainly of component B and the solvent, is directed to the solvent recovery column (C2). Here, component B is distilled off and collected as the overhead product, while the solvent is recovered at the bottom and recycled back to C1 for continuous operation.

Extractive distillation operates by leveraging solvent-induced modifications of liquid-phase nonidealities to enhance the relative volatility between components in a mixture. The added solvent selectively alters the activity coefficients of the key components, facilitating their separation. To achieve this effect, a sufficiently high solvent concentration within the column is required. The effectiveness of the process relies on several critical conditions:

1. **Selective interaction**: The solvent must exhibit differential interactions with the components to be separated, modifying their liquid-phase behavior in distinct ways. Without this selectivity, no meaningful enhancement in separability can be achieved.
2. **Low volatility**: The solvent must have a significantly higher boiling point than the target components and remain predominantly in the liquid phase throughout the extractive section. This ensures that the solvent is not lost with the distillate and that it effectively alters phase behavior where needed.
3. **No new azeotropes**: The solvent must not form additional azeotropes with any component of the original mixture, as this would introduce new separation challenges and compromise the overall process.
4. **Column configuration**: The extractive distillation column must be of a double-feed type, where the solvent is introduced above the main feed stage. This creates a distinct extractive section—situated between the rectifying and stripping zones—where the solvent influences the relative volatility.

Given these constraints, binary separation by extractive distillation is limited to systems that correspond to two types of three-component residue curve map topologies: those involving close-boiling (or pinched) mixtures and those forming minimum-boiling azeotropes.

The product compositions attainable in double-feed extractive distillation columns differ fundamentally from those achievable in single-feed columns. Specifically, for a given solvent, only one of the original binary components can be recovered as a pure distillate from the extractive column. In close-boiling systems, this component typically corresponds to the higher-boiling saddle point. In minimum-boiling azeotropic systems, both components may occupy saddle positions, and the solvent determines which component is displaced toward the distillate. Importantly, while a specific solvent will only favor one component for recovery, alternative solvents can shift the separation preference toward the other component. Simple screening tests exist to determine the distillate-selective behavior of a candidate solvent, as discussed later.

Finally, extractive distillation is most suitable for mixtures in which the components differ significantly in functional groups, as these molecular differences enhance the solvent's ability to differentiate and selectively interact with the species in the liquid phase.

2.1.1.1. Solvent Effects in Extractive Distillation

In conventional distillation of ideal or non-azeotropic mixtures, the component with the lower pure-component boiling point is consistently recovered in the distillate, while the higher-boiling component remains in the bottoms. However, this predictable behavior does not always hold in extractive distillation processes.

Depending on the nature of the solvent used, the separation behavior can vary significantly. With certain solvents, the distillate composition may follow the expected trend—recovering the lower-boiling component at the top of the column, as in standard distillation. However, for other solvents, the order may be reversed, and the higher-boiling component of the original mixture may instead be recovered in the distillate.

This reversal arises from the solvent's ability to selectively alter the activity coefficients of the components, thereby modifying their effective volatility. The resulting change in relative volatility is not governed solely by the components' vapor pressures, but also by how the solvent interacts with each species in the liquid phase.

In typical applications of extractive distillation, the original relative volatility between the light and heavy key components is often close to unity—indicating a very difficult separation under conventional means.

Assuming an ideal vapor phase and subcritical components, the relative volatility between the light and heavy keys of the desired separation can be written as the product of the ratios of the pure-component vapor pressures and activity coefficients whether the solvent is present or not:

$$\alpha_{L,H} = \left(\frac{P_L^{sat}}{P_H^{sat}}\right)\left(\frac{\gamma_L}{\gamma_H}\right) \qquad \text{(Eq.2.1.1.1)}$$

Where:
P_L^{sat} : Vapor pressure of light component
P_H^{sat}: Vapor pressure of heavy component
γ_L : Activity coefficient of light component
γ_H : Activity coefficient of heavy component

The addition of a high-boiling solvent in extractive distillation indirectly influences the vapor-pressure ratio of the key components by increasing the overall operating temperature of the column. This temperature elevation occurs because the solvent is introduced in relatively high molar proportions compared to the primary feed, and its low volatility results in a thermal shift upward relative to simple distillation of the same binary mixture—unless counteracted by a decrease in system pressure.

As a result, the vapor pressures of both components increase with temperature. However, this rise typically does not cause a significant change in relative volatility, since the vapor-pressure ratio tends to remain approximately constant—provided the vapor-pressure curves of the components exhibit similar slopes. Therefore, the "natural" volatility ordering of the components, as determined by their pure-component vapor pressures, is generally preserved.

In contrast, the dominant influence of the solvent arises from its effect on the activity coefficients of the components, which are highly sensitive to composition and molecular interactions in the liquid phase. The solvent modifies the non-ideality of the mixture by differentially affecting the activity coefficients of the components, depending on their chemical affinity and structural similarity to the solvent.

The key component that exhibits liquid-phase behavior similar to the solvent's tends to form a nearly ideal solution with it. Molecular interactions in this case are weak and non-specific, often leading to activity coefficients close to unity or even negative deviations from Raoult's law in the presence of solvating or complexing effects.

Conversely, the key component that is dissimilar to the solvent tends to undergo unfavorable interactions, leading to positive deviations from ideality. Its activity coefficient increases, especially under the diluting effect of a high solvent concentration. In some cases, the activity

coefficient may approach its infinite dilution value, which is typically large, further enhancing the effective volatility contrast between the two components.

Thus, the solvent acts as a selective molecular discriminator, suppressing the volatility of one component through idealization and amplifying the volatility of the other via increased nonideality—thereby enabling separations that would otherwise be infeasible using conventional distillation techniques.

The natural relative volatility of the system is enhanced when the activity coefficient of the lower-boiling pure component is increased by the solvent addition:

$$\gamma_L/\gamma_H \text{ increases and } \frac{P_L^{sat}}{P_H^{sat}} > 1 \qquad \text{(Eq.2.1.1.2)}$$

In this case, the lower boiling pure component will be recovered in the distillate as expected. For the higher-boiling pure component to be recovered in the distillate, the addition of the solvent must decrease the ratio γ_L/γ_H such that the product of γ_L/γ_H and P_L^{sat}/P_H^{sat} (that is $\alpha_{L,H}$) in the presence of the solvent is less than unity.

Recovering the higher-boiling component as the distillate in extractive distillation is typically more challenging and demands a higher solvent-to-feed ratio. Therefore, it is generally more practical to select a solvent that facilitates the separation of the lower-boiling component as the distillate.

There are several methods to predict which component will be recovered at the top of the extractive distillation column. One approach involves analyzing binary vapor–liquid equilibrium diagrams (y–x plots) without solvent. By incrementally increasing the solvent concentration, one can observe that, at a certain concentration, the azeotrope disappears at one of the pure-component ends. The component corresponding to that corner is the one that will be recovered in the distillate.

La Roche and colleagues (1991) proposed a graphical method using ternary diagrams[2]. In this method, a specific curve is plotted to indicate where the relative volatilities of the two components become equal. If this curve crosses the binary edge between the low-boiling component and the solvent, that component will appear in the distillate. Conversely, if the curve crosses the high-boiling component and solvent edge, the high-boiling component will be recovered overhead.

Another straightforward way to predict the separation behavior—if accurate residue curve maps are available—is to observe how the residue curves behave as they approach the solvent corner. The component toward which the curves tend indicates which key will remain with the solvent in the bottoms.

[2] La Roche, A., Doherty, M. F., & Malone, M. F. (1991). Separability characteristics of homogeneous azeotropic mixtures. *Canadian Journal of Chemical Engineering, 69*(5), 1302–1311. https://doi.org/10.1002/cjce.5450690514

Extractive Distillation Design and Optimization

Extractive distillation column composition profiles have a very characteristic shape on a ternary diagram. Stripping and rectifying profiles start at the bottoms and distillate compositions, respectively, track generally along the faces of the composition triangle, and then turn toward the high-boiling (solvent) node and low-boiling node, respectively, track generally along the faces of the composition triangle, and then turn toward the high-boiling (solvent) node and low-boiling node, respectively.

For a feasible single feed design these profiles must cross at some point. However, in an extractive distillation they cannot cross. The extractive section profile acts as the bridge between these two sections. Most of the key component separation occurs in this section in the presence of high solvent composition.

The variable that has the most significant impact on the economics of an extractive distillation is the solvent-to-feed flow rate ratio S/F. However, the extent of enhancement of the relative volatility is largely determined by the solvent composition in the lower column sections and hence the S/F ratio. The relative volatility tends to increase as the S/F ratio increases. This, a given separation can be accomplished in fewer equilibrium stages.

For the separation of a minimum-boiling binary azeotrope by extractive distillation, there is clearly a minimum-solvent flow rate below which the separation is impossible (due to the azeotrope). For azeotropic separations, the number of equilibrium stages is infinite at or below (S/F)min and decreases rapidly with increasing solvent feed flow, and then may asymptote, or rise slowly.

The relationship between the total number of stages and the S/F ratio for a given purity and recovery for the azeotropic acetone-methanol system with water as solvent. A rough idea of (S/F)min can be determined from a pseudobinary diagram or by plotting the $\alpha_{L,H} = 1$ line on a ternary diagram. The solvent composition at which the azeotrope disappears in a corner of the pseudobinary diagram or by plotting of the pseudobinary diagram is an indication of (S/F)min. An exact method for calculating (S/F)min is given by Knapp and Doherty [AIChE J. 40: 243 (1994)].

Typically, operating S/F ratios for economically acceptable solvents are between 2/r. Higher S/F ratios tend to increase the diameter of both the extractive column and the solvent recovery columns, but they tend to reduce the required number of equilibrium stages and minimum reflux ratio. Moreover, higher S/F ratios lead to higher reboiler temperatures, resulting in the use of higher-cost utilities, higher utility usages, and greater risk of degradation. Knight and Doherty [Ind. Eng. Chem. Fundam. 28: 564 (1989)] have published rigorous methods for computing minimum reflux for extractive distillation; they found that an operating reflux ratio 1,2 to 1,5 times the minimum value is usually acceptable. Interestingly, unlike other forms of distillation, in extractive distillation the distillate purity or recovery does not increase monotonically with increasing reflux ratio for a given number of stages.

At reflux ratios above the maximum (Rmax), separation becomes less effective, and the distillate purity actually decreases for a given number of stages [LaRoche et al., AIChE J. 38:1309 (1992)]. As the solvent-to-feed (S/F) ratio increases, the gap between the minimum (Rmin) and maximum reflux ratios widens. Excessive reflux reduces the solvent concentration in the top section of the column, which can impair performance rather than improve it. This means that the typical control strategy of increasing reflux to maintain purity may backfire when operating near or beyond Rmax. However, Rmax generally occurs at impractically high values and is rarely a concern in practice.

The thermal condition of the solvent feed does not influence the minimum S/F ratio, but it can affect the minimum reflux requirement—particularly at high S/F ratios. A colder (subcooled) upper solvent feed shifts Rmax to higher values, as it offers additional internal refluxing capacity, reducing the need for external reflux. Additionally, feeding the primary feed as a vapor can help maintain a higher solvent concentration on the feed tray and the trays below, enhancing separation.

Classical design references—such as Robinson and Gilliland (1950), Smith (1963), Van Winkle (1967), and Walas (1988)—provide detailed stage-to-stage design methods, along with shortcut and graphical techniques to determine key parameters like minimum stages, (S/F)min, and minimum reflux. More recent work by Knapp and Doherty [AIChE J. 40:243 (1994)] presents geometric and fixed-point methods to calculate (S/F)min, Rmin, and Rmax.

While most commercial simulators can handle heat and material balances for extractive distillation columns with multiple feeds, they typically lack direct tools to calculate (S/F)min and the minimum or maximum reflux ratios.

Solvent Screening and Selection

Choosing an effective solvent can have the most profound effect on the economics of an extractive distillation process. The approach most often adopted is to first generate a short list of potential solvents by using simple qualitative screening selection methods.

Experimental verification is best undertaken only after a list of promising candidate solvents has been generated and some chance at economic viability has been demonstrated via preliminary process modeling.

Solvent selection and screening approaches can be divided into two levels of analysis. The first level focuses on the identification of functional groups or chemical families that are likely to give favorable solvent-key component molecular interactions. The second level of analysis identifies and compares individual candidate solvents. The various methods of analysis are described briefly and illustrated with an example of choosing solvent for the methanol-acetone separation.

First level: Broad Screening by Functional Group

Homologous series. Select candidate solvents from the high-boiling homologous series of both light and heavy key components. Favor homologs of the heavy key because this tends to enhance the natural relative volatility of the system.
Homologous components tend to form ideal solutions and are unlikely to form azeotropes.

Robbins chart. Select candidate solvents from groups in the Robbins chart that tend to give positive (or no) deviations from Raoult's law for the key components desired in the distillate and negative (or no) deviations for the other key.

Hydrogen-bonding characteristics. Select candidate solvents from groups that are likely to cause the formation of hydrogen bonds with the key component to be removed in the bottoms, or disruption of hydrogen bonds with the key to be removed in the distillate. [Ewell et al , Ind. Eng. Chem. 36: 871 (1944); Gilmont et al ,Ind. Eng. Chem. 53: 223 (1961); Berg, Chem. Eng. Prog. 65(9): 52 (1969)].

Polarity characteristics. Select candidate solvents from chemical groups that tend to show higher polarity than one key component or lower polarity than the other key Polarity effects are often cited as a factor in causing deviations from Raoult's law [Hopkins and Fritsch, Chem. Eng. Prog. 51(8):(1954); Carlson et al , Ind. Eng. Chem. 46: 350 (1954); Prausnitz and Anderson, AIChE J. 7: 96 (1961)]. The general trend in polarity based on the functional group of a molecule is given in Table 13-19 The chart is best for molecules of similar size A more quantitative measure of the polarity of a molecule is the polarity contribution to the three-term Hansen solubility parameter. A tabulation of calculated three-term solubility parameters is provided by Barton (CRC Handbook of Solubility Parameters and Other Cohesion Parameters CRC Press, Boca Raton, Fla, 1991), along with a group contribution method for calculating the three-term solubility parameters of compounds not listed in the reference.*

Second level: Identification of Individual Candidate Solvents

Boiling point characteristics. Select only candidate solvents that boil at least 30 ºC to 40 ºC above the key components to ensure that the solvent is relatively nonvolatile and remains largely in the liquid phase. With this boiling point difference, the solvent should also not form azeotropes with the other components.

Selectivity at infinite dilution. Rank candidate solvents according to their selectivity at infinite dilution. The selectivity at infinite dilution is defined as the ratio of the activity coefficients at infinite dilution of the two key components in the solvent. Since solvent effects tend to increase as solvent concentration increases, the infinite-dilution selectivity gives an upper bound on the efficacy of a solvent. Infinite-dilution activity coefficients can be predicted by using such methods as UNIFAC, ASOG, MOSCED (Reid et al., Propertiesof Gases and Liquids, 4th ed., McGraw-Hill, New York, 1987).

Experimental measurements of relative volatility. Rank candidate solvents by the increase in relative volatility caused by the addition of the solvent. One technique is to experimentally measure the relative volatility of a fixed-composition, key component + solvent mixture (often a 1/1 ratio of each key, with a 1/1 to 3/1 solvent/key ratio) for various solvents.

In order to determine the best entrainer for the extractive distillation, a study of the pseudobinary equilibrium of the mixture was taken to term using *Aspen Properties*®. This was done using different fractions of entrainer.

The fundamentals behind the effect of entrainer presence in the mixture and how it affects equilibrium is due to the fact that entrainers that have high boiling points interact with the liquid phase, altering the vapor-liquid equilibria; however, due to their high temperature of evaporation, they do not transfer to the vapor phase. Ultimately, what is affected by the presence

of the entrainer is the relative volatility of the components in the mixture, making the separation more feasible.

Different substances create interactions with the mixtures that allow separation by distillation to be more feasible by making the components easier to be separated.

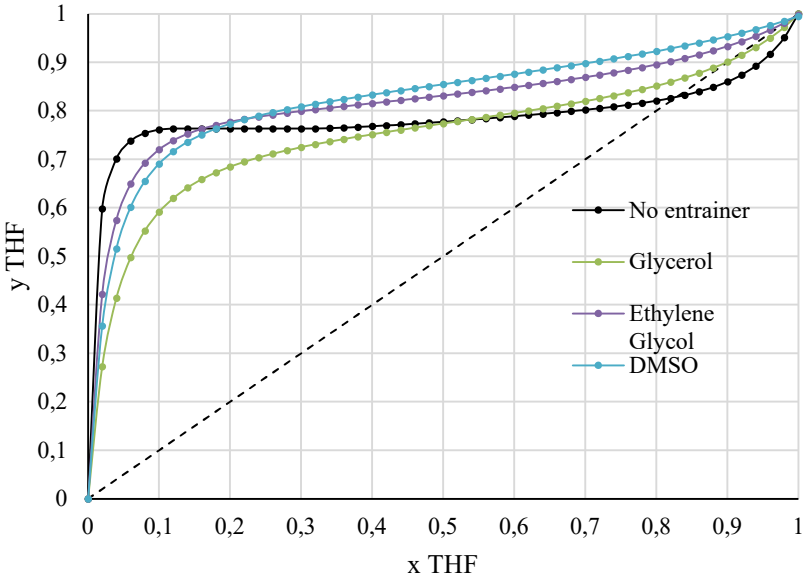

Figure 2.1.1.1.1. Pseudobinary VLE x-y diagram for mixture THF(1)/Water(2) for 1 atm with a 0,2 fraction of entrainer.

By changing the activity coefficients of the liquid mixtures, the azeotrope disappears from the mixture, however, DMSO and Ethylene Glycol both show a higher ability to separate the azeotrope. Therefore, these are preferred.

Extractive Distillation Design

Confidential information

Confidential information

2.1.2. **Exploiting Pressure Sensitivity**

Breaking a homogeneous azeotrope located along a distillation boundary requires the separation process to "cross" that boundary. This can be accomplished by introducing an external stream to shift the feed composition into a different distillation region amenable to separation.

However, the added stream must be fully regenerated to maintain mass balance. Simply recycling one of the product streams does not qualify as a valid method for breaking a homogeneous binary azeotrope.

An alternative method involves exploiting pressure sensitivity—if the azeotropic composition and corresponding distillation boundary shift appreciably with pressure. A composition that lies in one distillation region at pressure P1 may move to another region at pressure P2.

Consider, for example, a pressure-swing distillation system for separating a binary maximum-boiling azeotrope. At pressure P1, the azeotrope is richer in component B than at pressure P2. The first column operates at P1 and receives a feed composed of fresh input and recycled bottoms from the second column. This combined feed is adjusted to lie on the A-rich side of the azeotrope at P1, allowing recovery of pure A as distillate, while the bottoms approach the azeotropic composition.

The bottoms are then flashed or compressed to P2 and introduced into the second column. At this pressure, the composition falls on the B-rich side of the azeotrope. Pure B is collected as distillate, and the bottoms—now near the azeotropic composition—are recycled to the first column.

A similar flowsheet can be applied to homogeneous minimum-boiling azeotropes. In such cases, both columns produce the pure components as bottom products, while the azeotropic distillates are cross-recycled.

For pressure-swing distillation to be viable, the azeotropic composition must shift by at least 5%—preferably 10% or more—over a moderate pressure difference (typically less than 10 atm). Larger pressure differences can introduce complications such as the need for refrigeration of low-pressure distillates or excessive reboiler duty at high pressures.

If the composition shift is minimal, recycle flow rates must be increased substantially. This is especially problematic for minimum-boiling azeotropes, where the overheads from both columns must be recycled, leading to high energy consumption and large capital investment due to oversized equipment.

Furthermore, one lobe of the azeotropic VLE diagram may remain pinched regardless of pressure, necessitating a large number of stages in at least one column to achieve high purity.

Ultimately, only a limited subset of azeotropes exhibit sufficient pressure sensitivity for pressure-swing distillation to be economically feasible. One notable example is the tetrahydrofuran–water minimum-boiling azeotrope. [Tanabe et al ; U S Patent 4,093,633 (1978)].

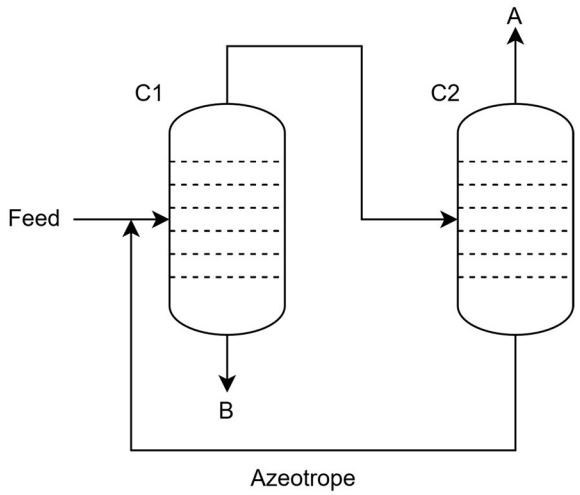

Figure 2.1.2.1. Feasible distillation region diagrams and associated distillation system for breaking a homogeneous minimum-boiling binary azeotrope A-B. Component B boils at a higher temperature than does A.

Despite, Tetrahydrofuran/Water mixture being known as one of the very few separations that allow Pressure Swing Distillation as a feasible operation in order to purify THF, in our process is not viable due to the fact that due to Process Safety limitations the pressures that allow an economically profitable separation (according to the TAC) are out of the range of operation.

Following a detailed evaluation of this separation strategy, it was confirmed that the azeotropic mixture exhibits a significant degree of pressure sensitivity. Specifically, operating the system under vacuum conditions resulted in a measurable shift in the azeotropic composition. This shift enabled effective separation of the components, particularly allowing for the enrichment of tetrahydrofuran (THF) in the distillate stream. Consequently, it became feasible to achieve a high-purity THF product without resorting to more complex and capital-intensive multi-column configurations such as extractive or azeotropic distillation systems. This not only simplifies the overall process design but also reduces both equipment footprint and operational costs, making the proposed vacuum-based separation an efficient and economically attractive alternative.

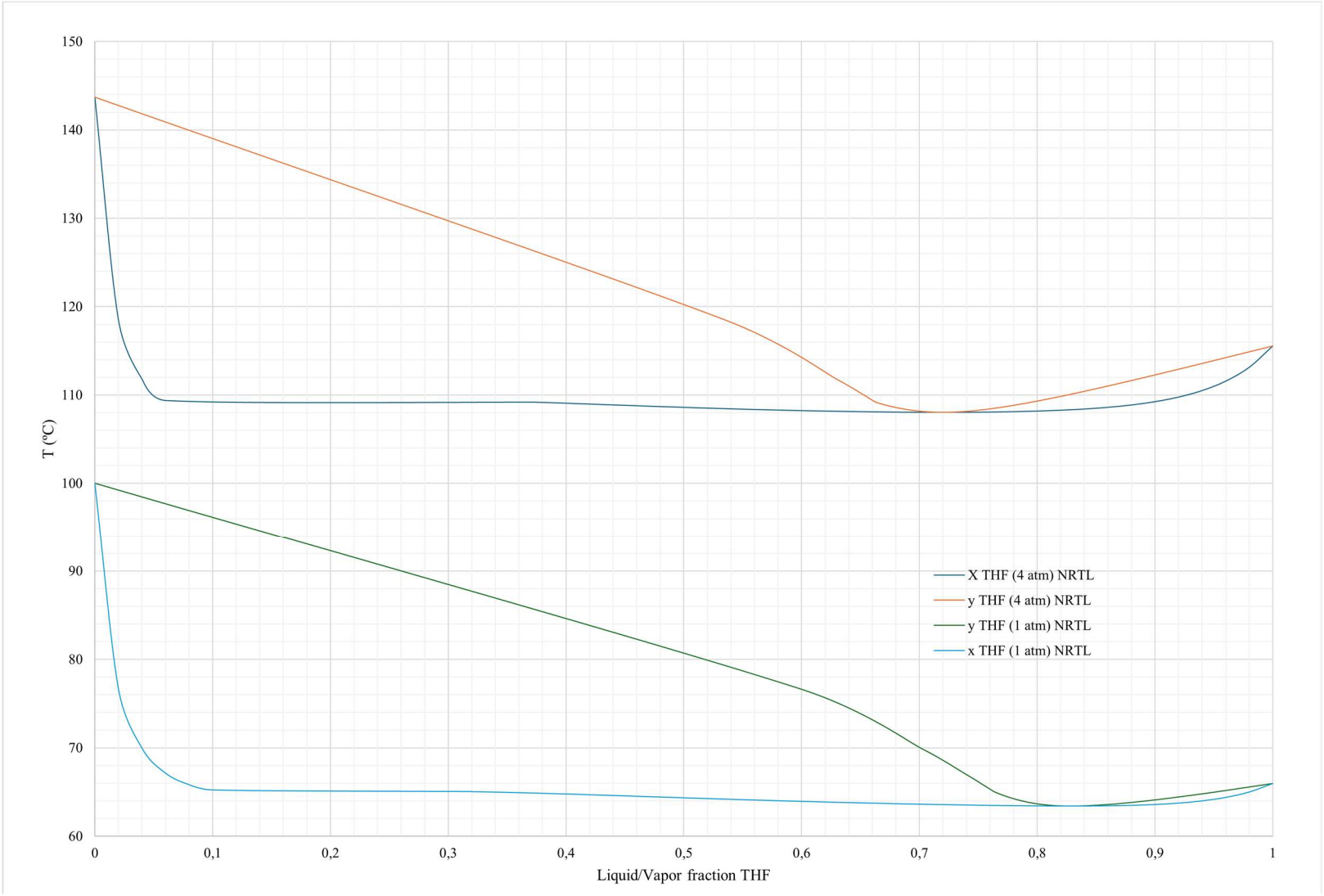

Figure 2.1.2.2. Binary equilibrium diagram for THF/Water mixture for two pressures (1 atm and 4 atm)

3. TECHNOLOGY DEVELOPMENT AND PROCESS MODELLING

The integration of technology development and process modelling plays a critical role in the design, optimization, and scale-up of chemical processes. Through the use of advanced thermodynamic models, kinetic studies, and simulation tools, it becomes possible to evaluate process feasibility, predict system behavior, and identify optimal operating conditions with greater precision and efficiency. In this section, a systematic approach to process development is presented, combining experimental data with rigorous modelling techniques to guide decision-making and support the implementation of robust, scalable, and economically viable industrial solutions.

3.1. Thermodyamic model selection

In order to achieve an accurate design through simulation, a thermodynamic model that is able to represent the real behavior of the substances under operating conditions is necessary. The thermodynamic model is the framework that describes the behavior and properties of a physical system in terms of our state variables.

As stated previously, in Section 2, the vapor-liquid equilibrium behavior of the mixture of tetrahydrofuran and water is highly non ideal, showing azeotropic behavior. When selecting the method for thermodynamic properties calculation using Aspen, what the software does is that it uses two methods of calculating vapor-liquid equilibrium, through the equation-of-state method and the activity coefficient method. Each method contains the following:

- Fundamental concepts of phase equilibria and the equations used
- Application to vapor-liquid equilibria
- Calculation of other thermodynamic properties

The key thermodynamic property calculation performed is phase equilibrium. The basic relationship for every component *I* in the vapor and liquid phases of a system at equilibrium is:

$$f_i^v = f_i^l \qquad \text{(Eq. 3.1.1)}$$

Where:
f_i^v: Fugacity of component *i* in the vapor phase
f_i^l: Fugacity of component *i* in the liquid phase

Each property method in the Aspen Physical Property System is based on either the equation-of-state method or the activity coefficient method for phase calculations. The phase equilibrium method determines how other thermodynamic properties such as enthalpies and molar volumes are calculated.

Equation of state method (EOS)

In this method, a coefficient is used to describe the fugacity of the component *i* in its' different phases.

$$\ln \varphi_i^{\alpha} = -\frac{1}{RT}\int_{\infty}^{V\alpha}\left[\left(\frac{\partial p}{\partial n_i}\right)_{T,V,n_i} - \frac{RT}{V}\right]dV - \ln Z_m^{\alpha} \quad \text{(Eq. 3.1.2)}$$

Where:
α: Phase (vapor or liquid)
V: Total volume
n_i: Mole number of component *i*

This coefficient is applied to describe the fugacity in the following expressions:

$$f_i^v = \varphi_i^v y_i p \quad \text{(Eq. 3.1.3)}$$
$$f_i^l = \varphi_i^l y_i p \quad \text{(Eq. 3.1.4)}$$

Some examples of available models for simulation that use this method are: Redlich-Kwong-Soave (SRK), Peng-Robinson (PR) and/or Lee-Kesler-Plöcker (LKP).

Activity coefficient method

In this calculation, the fugacity of the vapor phase is calculated using Eq. 3.1.3. However, the fugacity of the liquid phase is calculated using:

$$f_i^l = x_i \Upsilon_i f_i^{*,l} \quad \text{(Eq. 3.1.5)}$$

Where:
Υ_i: Liquid activity coefficient of component *i*
$f_i^{*,l}$: Liquid fugacity of pure component *i* at mixture temperature

With an equation-of-state method, all properties can be derived from the equation of state, for both phases. Using an activity coefficient method, the vapor phase properties are derived from an equation state, exactly as in the equation-of-state method. However, the liquid properties are determined from summation of the pure component properties to which a mixing term or an excess term is added. The activity coefficient represents the deviation of the mixture form ideality.

The activity coefficient is the best way to represent highly non-ideal liquid mixtures at low pressures. You must estimate or obtain binary parameters from experimental data, such as phase equilibrium data. Binary parameters for the Wilson, NRTL and UNIQUAC models are available in the the Aspen Physical Property System for a large number of component pairs.

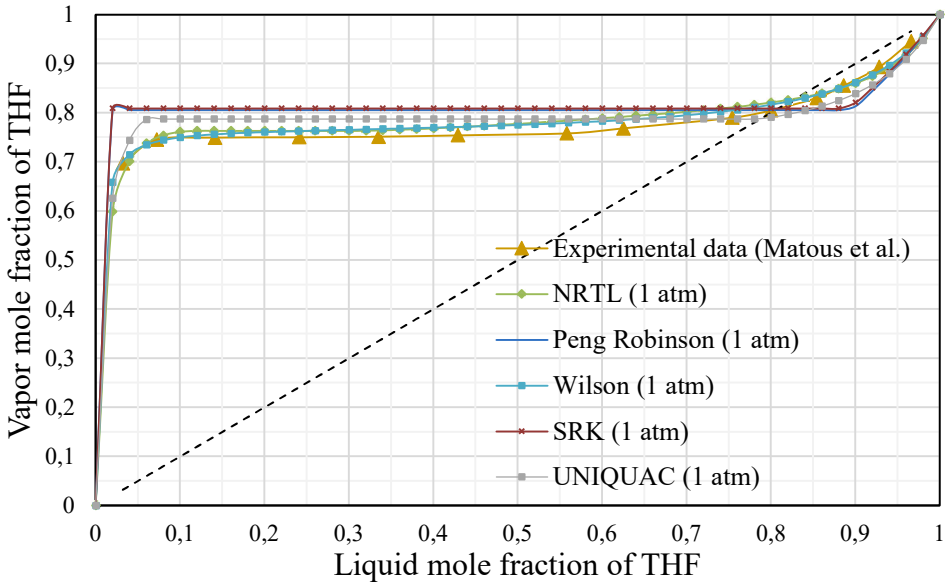

Figure 3.1.1. VLE for binary mixture THF(1)/Water(2)

Taking this factor into account, the criterion for selecting the best thermodynamic model will be how close the results for the model are to the real experimental data for the mixture.

The models that show the greatest deviation from the experimental data are the Soave-Redlich-Kwong (SRK) and Peng-Robinson equations of state. In contrast, the UNIQUAC model provides a closer approximation, although it is less accurate than the NRTL and Wilson models, both of which yield results that closely align with the experimental data.

From representing these results, it's visible that the models that are the closer are the Wilson, NRTL and UNIQUAC, which is explained by the activity coefficient model. In order to compare the differences between these models, the Normalized Root Mean Square Error (nRMSE) by range will be used.

The RMSE is a standard statistical measure used to assess the accuracy of a model's prediction. It quantifies the difference between values predicted by a model and the actual observed values, serving as an indicator of model performance. It is calculated according to the following expression:

$$RMSE = \sqrt{\frac{1}{n}\sum_{i=1}^{n}\left(y_{THF,model}^{(i)} - y_{THF,empirical}^{(i)}\right)^2} \qquad \text{(Eq. 3.1.6)}$$

In this case, the normalized version will used to simplify the comparison between datasets with different scales.

$$nRMSE = \frac{RMSE}{\max\left(y_{THF,empirical}^{(i)}\right) - \min\left(y_{THF,empirical}^{(i)}\right)} \qquad \text{(Eq. 3.1.7)}$$

After applying this method to the most visibly accurate models (Wilson, NRTL and UNIQUAC) via solving a MATLAB code (see Annex A.1) the following results have been obtained:

Table 3.1.1. nRMSE Analysis results

Model	Value
Wilson	0,0504
NRTL	0,0729
UNIQUAC	0,1124

A results for the nRMSE that indicates accurate results could depend on the context, but overall a result lower than 10%, in this case, 0.1 means that the model is a good fit. Therefore, the Wilson model is the best; however, according to bibliography in simulations of THF/Water mixtures the NRTL is used more commonly. Due to how small the difference between the models is, both are considered accurate and appropriate to simulate the behavior of the THF/Water binary mixture.

In this case, the NRTL will be used to simulate the THF Recovery Unit.

3.2. Technology selection

Technology selection is a fundamental step in the development of efficient and economically viable industrial processes. It involves the systematic evaluation and comparison of available process alternatives based on technical performance, scalability, energy efficiency, environmental impact, and cost-effectiveness. This phase ensures that the chosen technology aligns with the operational objectives, regulatory requirements, and long-term sustainability goals of the project. In this section, a structured methodology is applied to assess and justify the selection of the most suitable separation technology for the process under study, supported by experimental data, modelling results, and feasibility criteria. The different available technologies have been presented in Section 2.

3.2.1. Initial Approach

As explained in section 2.1.1.1., the initial aim for the recovery unit was to acquire pure THF. Initially, this was thought to be the best approach in terms of applications *[Confidential information]*

However, studies about the solubility of pharmaceutical products in presence of solvents (Crafts, 2007, p. 43, Figure 7) proved otherwise[3].

[3] **Crafts, P.** (2007). The role of solubility modeling and crystallization in the design of active pharmaceutical ingredients. In K. M. Ng, R. Gani, & K. Dam-Johansen (Eds.), *Chemical product design: Toward a perspective through case studies* (Chapter 2). Elsevier.

Confidential information

3.2.2. Final Technology Selection

As previously demonstrated, the system's pressure sensitivity enabled the effective recovery of high-purity tetrahydrofuran (THF), achieving concentrations exceeding 75% under vacuum conditions. Consequently, the selected separation strategy was azeotropic distillation operated at reduced pressure (200 mbar), which proved to be the most technically and economically viable method for separating THF from water. *Confidential information*. As a result, the final process design was based on a binary distillation system.

3.2.2.1. Column Design

In this study, the McCabe-Thiele method is applied to design a distillation column for the separation of a water-THF binary mixture. The objective is to achieve a high-purity separation of the components while minimizing energy consumption and capital costs. By constructing the McCabe-Thiele diagram, key design parameters such as the number of stages, reflux ratio, and feed stage placement are determined. The results will provide a detailed understanding of the distillation process, guiding the design of an efficient and cost-effective separation system for water and THF.

The following sections will describe the theoretical background of the McCabe-Thiele method, the procedure for constructing the diagram, and the analysis of the results to optimize the distillation column design for the water-THF separation.

The McCabe-Thiele method is a graphical method that is based on the representation of material balance equations as operating lines on the x-y diagram. representation of material balance equations as operating lines on the x-y diagram.

- The liquid-phase flow rate as well as the vapor rate are assumed to be constant from tray to tray in each section of the column between feed and product points, in the case of the packed column, that would constant flow through the bed.
- Constant pressure
- Total condenser at the top of the column.

In the year 1925, McAbe and Thiele developed a graphical solution method for binary that consisted of representing the operating equations for this type of distillation as straight lines on the x-y diagram of binary mixtures.

This allowed to see how the equilibrium relation can be solved from the y-x equilibrium curve and the mass balances from the operating lines.

To see the different equations solved in the McAbe-Thiele see Annex A.1, the result was the following McAbe-Thiele diagram.

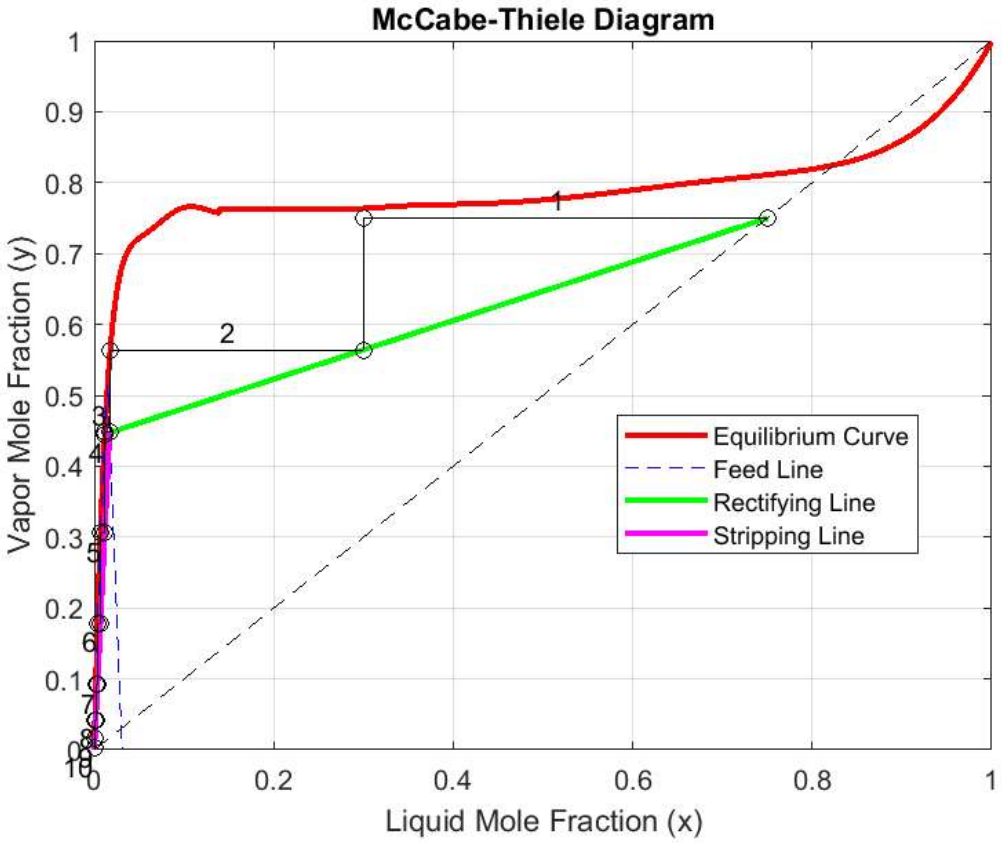

Figure 3.2.2.1.1. McCabe-Thiele Diagram (Graphical Method) using MATLAB.

Table 3.2.2.1.1. Binary distillation results

Parameter	Value
Quality of feed (q)	0,97
Minimum reflux ratio	0,47
Actual reflux ratio	0,7
Distillate flow rate (kmol/hr)	3,39
Bottoms flow rate (kmol/hr)	81,45
Light key recovery (%)	99,36
Heavy key recovery (%)	1,03
Total theorical stages	10
Actual stages	17
Optimal feed stage	3

Basic column design DSTWU

The DSTWU method (Distillation Short-Cut with Underwood Equations) is a shortcut method available in many process simulators (Aspen Plus, Aspen HYSYS, e.g.) that allows the preliminary design of distillation columns.

This simulation model allows the determination of key parameters design by specifying the following inputs:

- Recovery of the light and heavy keys
- Reboiler and condenser pressures
- Either reflux ratio or number of theoretical stages
- Condenser specifications

The theory behind this model is according to different equations used in short-cut calculations for binary distillations:

- **Winn's method**

This equation is used to determine the minimum number of theorical stages (Nmin). It is particularly useful for binary or nearly binary systems and is often employed in cases where the distillation process is not operating under total reflux.

$$N_{min} = \frac{\log\left(\frac{\frac{x_D}{1-x_B}}{\frac{x_B}{1-x_D}}\right)}{\log\left(\frac{\alpha_{LK}}{\alpha_{HK}}\right)} \qquad \text{(Eq. 3.2.2.1.1.1)}$$

Where:
x_D = mole fraction of light key in the distillate
x_B = mole fraction of the light key in the bottoms
α_{LK} = relative volatility of light key with respect to the heavy key
α_{HK} = relative volatility of heavy key with respect to the light key

This expression has the limitation that it assumes constant relative volatility and an ideal separation. The key assumptions of this method are the following:

1. Constant relative volatility: the relative volatility between the components is assumed to remain constant across the column
2. Binary or nearly binary mixture: the method works best when only two components dominate the separation process
3. Total reflux: Winn's method generally applies when considering the minimum number of stages when all the vapor is condensed and no distillate is withdrawn

Unlike the popular shortcut distillation design method FUG (Fenske-Underwood-Gilliland) this method allows a more detailed consideration of the feed condition and non-idealities, whereas the Fenske equation assumes total reflux along with ideal conditions.

Underwood Equations

The following expressions are used to calculate the minimum reflux ration R_{min} for a given separation, assuming an infinite number of stages. The Underwood method involves determining the root of the equation (θ) that satisfies the following equation:

Determination of parameter θ

$$\sum_i \frac{q-z_i}{\alpha_i-\theta} = 1-q \qquad \text{(Eq. 3.2.2.1.1.2)}$$

Where:
q = quality of the feed (fraction of feed that is liquid, 1 for liquid feed, 0 for vapor feed)
z_i = mole fraction of component *i* in the feed
α_i = relative volatility of component *i* with respect to heavy key
Θ = root of equation to solve numerically

Determination of minimum reflux ratio

Once the root of equation of Underwood has been found, the minimum reflux ratio can be calculated according to the following expression:

$$R_{min} = \sum_i \frac{x_D^i}{\alpha_i - \theta} \qquad \text{(Eq. 3.2.2.1.1.3)}$$

Where:
x_D^i = mole fraction of component *i* in the distillate

- **Gilliland Correlation**

The Gilliland correlation is an empirical relationship used to estimate the actual number of theorical stages (N) based on the minimum number of stages N_{min} and the actual reflux ratio R. The correlation relates to the dimensionless ratio of actual stages to minimum stages as a function of the ratio of the actual reflux to minimum reflux:

$$\frac{N - N_{min}}{N+1} = 0{,}75 \cdot \left(1 - \frac{R_{min}}{R}\right)^{0{,}566} \qquad \text{(Eq. 3.2.2.1.1.4)}$$

Where:

N = actual number of theorical stages
N_{min} = minimum number of theorical stages, determined using Fenske equation
R_{min} = minimum reflux ratio, determined from Underwood equation
R = actual reflux ratio

DSTWU Column Design

The shortcut method design DSTWU for our column is used in order to determine different important design parameters that will be used later on for the design of the RADFRAC model column; which a calculation block more complex.

Confidential information

Aspen Plus V14 DSTWU Column design (without pre-heating)

Confidential information

Aspen Plus V14 DSTWU Column design (with pre-heating)

The same analysis taken to term before will be repeated to study what is the effect of the feed thermal state to the separation.

The feed thermal state describes the condition of the feed stream entering the distillation column in terms of its phase and energy content. The thermal state or feed quality (q), determines how much of the feed is liquid or in vapor, which in turn influences the energy requirements in the column, the reflux ratio and the number of stages required for separation. This parameter follows the next expression:

$$q = \frac{H_{liquid} - H_{feed}}{H_{liquid} - H_{vapor}} \quad \text{(Eq.3.2.2.1.1.5)}$$

Where:

H_{feed} = is the enthalpy of the feed stream
H_{liquid} = is the enthalpy of the feed at its saturated liquid state
H_{vapor} = is the enthalpy of the feed at its saturated vapor state

Depending on the thermal state of the feed mixture to the column, different effects on the energy requirements of the equipment can be observed.

Table 3.2.2.1.5. Thermal state of the feed and effect on the colum

Quality factor	State	Impact on column
q > 1	Subcooled liquid, feed enters below boiling point	Increase of reboiler duty to bring feed to boiling point
q = 1	Saturated liquid, feed enters entirely liquid at boiling point	Reboiler duty is moderate, lower optimal reflux ratio
0 < q < 1	Partially vaporized, feed enters the column as a mixture of liquid and vapor	Low reboiler duty, high condenser duty, lower reflux ratio
q = 0	Saturated vapor, feed enters entirely as vapor at its dew point	Lower reboiler duty, higher condenser duty, higher reflux ratio
q < 0	Superheated vapor, feed enters vaporized about dew point	Highest condenser duty, higher reflux ratio, lowest reboiler duty

In order to study the effect of the thermal state in the simulation, a heat exchanger has been decided to add heat to the feed mixture. This allows to choose the feed state to the column while also determine the necessary heat duty for these conditions.

Confidential information

Aspen Plus V14 DSTWU Comparison and optimization

Confidential information

Aspen Plus V14 RADFRAC Column design

Confidential information

Model Design RADFRAC basic simulation

Confidential information

Model Design RADFRAC Column Internals

Confidential information

4. DESIGN: COLUMN WITH CONDENSER AND REBOILER

Confidential information

Confidential information

Confidential information

Confidential information

Confidential information

Confidential information

5. ECONOMICAL IMPACT EVALUATION

Confidential information

Given the scale of savings, the recovery column offers a rapid return on investment (ROI) while improving the environmental footprint and resource efficiency of the process.

Confidential information. According to the Carbon Footprints of Recycled Solvents study by the European Solvent Recycler Group (ESRG, 2013), the production of virgin THF emits approximately 5.73 tonnes of CO_2 per tonne, while recycled THF emits only 0.65 tonnes of CO_2 per tonne, resulting in a net savings of 5.08 tonnes of CO_2 per tonne of THF recovered.

Applied to the hourly recovery rate, this corresponds to a CO_2 emissions reduction of approximately 0,738 tonnes per hour. These avoided emissions reflect the upstream environmental impact of virgin solvent production—including raw material extraction, energy-intensive synthesis, and distillation—which is eliminated through in-house solvent recovery. As such, the system delivers not only operational and cost benefits, but also a substantial, quantifiable contribution to hourly decarbonization performance and the site's broader climate targets.

6. CONCLUSIONS

This thesis has evaluated the technical performance and environmental benefits of implementing a THF (tetrahydrofuran) recovery column within an industrial chemical production process. Through process data analysis and mass balance calculations, it was demonstrated that the column is capable of recovering approximately *[Confidential information]* kg of THF per hour, amounting to *[Confidential information]* tonnes of solvent per year under standard operating conditions. Additionally, the system enables the recovery of over *[Confidential information]* kg of clean water per hour from the bottom stream of the column, further enhancing the plant's material efficiency. These recoveries significantly reduce the demand for virgin solvent and fresh demineralized water, leading to operational cost savings and reduced waste generation.

Beyond the operational benefits, the environmental impact of the recovery system has been quantified using life cycle emissions data. According to the *Carbon Footprints of Recycled Solvents* study by the European Solvent Recycler Group (2013), virgin THF production emits approximately 5.73 tonnes of CO_2 per tonne, while recycled THF emits only 0.65 tonnes. By avoiding the production of virgin THF, the system achieves a net emissions reduction of 5.08 tonnes of CO_2 per tonne recovered, which translates to 0.738 tonnes of CO_2 avoided per hour, or nearly 5,900 tonnes per year. These avoided emissions reflect the upstream burdens of solvent synthesis, including fossil feedstock extraction, catalytic hydrogenation, and high-energy distillation—burdens that are eliminated when the solvent is reused in a closed-loop system.

The THF recovery system represents a tangible application of circular economy principles in the chemical industry. Instead of relying on a linear model—where solvents are purchased, used once, and disposed of—this process promotes a closed-loop system in which high-value materials are reclaimed and reintegrated into the production cycle. This reduces the extraction of virgin resources, minimizes hazardous waste generation, and alleviates pressure on water and energy systems. By extending the lifecycle of solvents, the recovery column directly contributes to improving the sustainability profile of the plant and supports long-term environmental stewardship.

However, while the environmental benefits of the recovery system are evident and substantial, the economic feasibility of the technology requires further investigation. This thesis focused on operational savings and emission reductions, but a complete financial assessment should also include capital expenditure (CAPEX), installation costs, maintenance, energy consumption of the recovery system, and any required auxiliary infrastructure. A detailed cost-benefit analysis and payback period calculation are essential to determine the speed at which the investment can be recovered and whether additional process optimizations or policy incentives (e.g., carbon credits or eco-tax savings) could accelerate profitability.

In conclusion, solvent recovery stands out as a technically effective and environmentally responsible strategy to reduce emissions, conserve resources, and improve process circularity. With further research into implementation costs and potential integration with broader sustainability frameworks, such systems have the potential to become standard practice in modern chemical production, aligning industrial performance with the growing demand for climate resilience and circular economy principles.

7. BIBLIOGRAPHY

1) Barton, A. F. M. (1991). *CRC handbook of solubility parameters and other cohesion parameters* (2nd ed.). CRC Press.
2) BASF. (n.d.). *Historia de BASF en España*. BASF. Retrieved January 30, 2025, from https://www.basf.com/es/es/who-we-are/BASF-en-Espan-a/Historia
3) Berg, L. (1969). Solvent selection: A solvency parameter approach. *Chemical Engineering Progress*, *65*(9), 52–58.
4) Carlson, E. C., Eckert, C. A., & Dekker, E. E. (1954). Solubility parameter correlation. *Industrial & Engineering Chemistry*, *46*, 350–355.
5) Chávez Velasco, J. A., Tawarmalani, M., & Agrawal, R. (n.d.). *Which separation scenarios are advantageous for membranes or distillations?* [Manuscript or report].
6) Clark, D. E. (2001). Peroxides and peroxide forming compounds. *Chemical Health & Safety*, *8*(5), 12–21.
7) Ewell, R. H., Harrison, B. F., & Berg, L. (1944). Extractive distillation. *Industrial & Engineering Chemistry*, *36*, 871–875.
8) Gilmont, G. R., & Walton, H. F. (1961). Tetrahydrofuran–water systems. *Industrial & Engineering Chemistry*, *53*, 223–228.
9) Hamad, A., & Dunn, R. F. (n.d.). *Energy optimization of pressure-swing azeotropic distillation systems*. American University of Sharjah / McSwain Engineering, Inc.
10) Hopkins, R. B., & Fritsch, M. A. (1954). Extractive distillation practice. *Chemical Engineering Progress*, *51*(8).
11) Jackson, H. L., McCormack, W. B., Rondestvedt, C. S., Smeltz, K. C., & Viele, I. E. (1970). Peroxides in organic solvents. *Journal of Chemical Education*, *47*(3), A175–A188.
12) Kelly, R. J. (1996). Review of safety guidelines for peroxidizable organic chemicals. *Chemical Health & Safety*, *3*(5), 28–36.
13) Knapp, J. P., & Doherty, M. F. (1994). Thermodynamic analysis of reactive azeotropy. *AIChE Journal*, *40*(2), 243–268.
14) LaRoche, R. D., Doherty, M. F., & Malone, M. F. (1992). Separation of azeotropic mixtures by homogeneous azeotropic distillation. *AIChE Journal*, *38*(8), 1309–1321.
15) Lee, J., Cho, J., Kim, D. M., & Park, S. (n.d.). Separation of tetrahydrofuran and water using pressure swing distillation: Modeling and optimization. [Article or conference paper; publication details incomplete].
16) Martínez Lara, J., Martínez Lara, B. A., Serna González, M., & Castro Montoya, A. J. (n.d.). *Simulation of separation of tetrahydrofuran–water by extractive distillation with glycerol*. Universidad Michoacana de San Nicolás de Hidalgo.
17) National Safety Council. (1987). *Recognition and handling of peroxidizable compounds* (Data Sheet I655-Rev. 87). National Safety Council.
18) Prausnitz, J. M., & Anderson, T. F. (1961). Correlation of vapor-liquid equilibria by the UNIFAC method. *AIChE Journal*, *7*, 96–104.
19) Robinson, C. S., & Gilliland, E. R. (1950). *Elements of fractional distillation* (3rd ed.). McGraw-Hill.
20) Royal Society of Chemistry. (2015). *Peroxides formation from tetrahydrofuran (THF)*. Retrieved from https://pubs.rsc.org/en/content/articlelanding/2015/OB/C5OB00012B#!divAbstract
21) S&P Global Commodity Insights. (n.d.). *VLE phase diagram, residue curve map*. Retrieved from https://vle-calc.com

22) Seader, J. D., Henley, E. J., & Roper, D. K. (2011). *Separation process principles* (3rd ed.). Wiley.
23) Simulation of the tetrahydrofuran dehydration process by extractive distillation in Aspen Plus. (2007). *Proceedings of the European Congress of Chemical Engineering (ECCE-6)*, Copenhagen, Denmark, 16–20 September 2007.
24) Smith, B. D. (1963). *Design of equilibrium stage processes*. McGraw-Hill.
25) Tanabe, K., et al. (1978). *Separation of tetrahydrofuran and water by extractive distillation* (U.S. Patent No. 4,093,633). U.S. Patent and Trademark Office.
26) Van Winkle, M. (1967). *Distillation*. McGraw-Hill.
27) Walas, S. M. (1988). *Chemical process equipment: Selection and design*. Butterworths.
28) Aspen Technology, Inc. (n.d.). *Aspen Plus user guide* [Software documentation].

ANNEXES

A.1. MCCABE-THIELE METHOD USING MATLAB

Building the code is the methodology for determining the basis of design of the binary separation. Some of the equations that are used are the following:

EQUILIBRIUM RELATIONS

$$y = \frac{\alpha \cdot x}{1-(1-\alpha)\cdot x} \quad \text{(A.1.1)}$$

$$x = \frac{y}{1+(1-\alpha)\cdot y} \quad \text{(A.1.2)}$$

TOP SECTION LINE

$$y = \frac{R}{1+R} \cdot x + \frac{x_D}{1+R} \quad \text{(A.1.3)}$$

BOTTOM SECTON LINE

$$y' = \frac{L'}{V'}x' - \frac{B}{V'}x_W{}' \quad \text{(A.1.4)}$$

Q-LINE

$$y = \frac{q}{q-1}x_i - \frac{1}{q-1}x_F \quad \text{(A.1.5)}$$

Procedure for calculation:

1. Finding an equation for the equilibrium relation through data fitting tool.

In order to build the code, the equilibrium relations between the vapor phase and the liquid phase are necessary, therefore, the first thing that has been is to find this relationship by studying the behavior of the VLE data.

Due to the fact that the VLE is non ideal, finding a function that describes the behavior of the mixture is more complicated. Therefore, the procedure that is going to be used is to fit the data using the Data Fitting Tool of *MatLab*®.

As stated in Section 3.1., the vapor liquid data of Aspen Plus databanks, resembles significantly the real behavior of the mixture, therefore, this has been used in order to extract the mathematical expressions that describe the non ideal behavior of the mixture.

Due to the difficulty of finding a unique polynomial expression that allows describing the behavior of the function, the data has been split into sections to find adjustments that allow a good coefficient of determination. This parameter determines the quality of the model in replicating the results.

First section fitting

The first section fitting function (y_1) is the following:

$$y_1(x) = 4{,}8851 \cdot 10^6 \cdot x^7 - 4{,}2504 \cdot 10^6 \cdot x^6 + 1{,}5078 \cdot 10^6 \cdot x^5 - 2{,}8073 \cdot 10^5 \cdot x^4 + 2{,}9444 \cdot 10^4 \cdot x^3 - 1{,}7393 \cdot 10^3 \cdot x^2 + 54{,}7078 \cdot x \quad \text{(A.1.6)}$$

Second section fitting

The second section fitting function (y_2) is the following:

$$y_2(x) = -2{,}3933 \cdot 10^{-15} \cdot x + 0{,}7633 \quad \text{(A.1.7)}$$

Third section fitting

$$y_3(x) = 17{,}5661 \cdot x^5 - 50{,}3215 \cdot x^4 + 56{,}0001 \cdot x^3 - 30{,}0252 \cdot x^2 + 7{,}8025 \cdot x - 0{,}0233 \quad \text{(A.1.8)}$$

The statistical accuracy results are the following:

Table A.1.1. Goodness of Fit result

Parameter	**y_1**	**y_2**	**y_3**
SSE	0,0002	0,0000	0,0001
R^2	0,9996	-	0,9990
DFE	4,0000	3,0000	7,0000
Adjusted R^2	0,9988	-	0,9983
RMSE	0,0074	0,0000	0,0028

The fitting result can be seen in the following figure

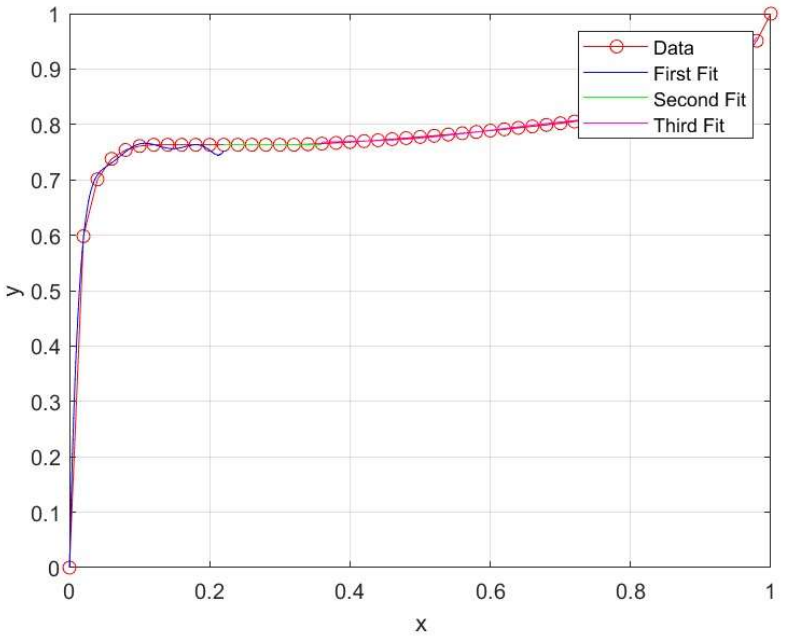

Figure A.1.1 Data with fitted polynomial expression plotted.

The combined function $y_{eq}(x)$ defined piecewise as:

$$y_{eq}(x) = \begin{cases} y_1(x), & for\ 0 \leq x \leq 0{,}14 \\ y_2(x), & for\ 0{,}14 < x \leq 0{,}3 \\ y_3(x), & for\ 0{,}3 < x \leq 1 \end{cases} \quad \text{(A.1.9.)}$$

In order to observe how well this models adjusts to the data, we can see the following figure with the model:

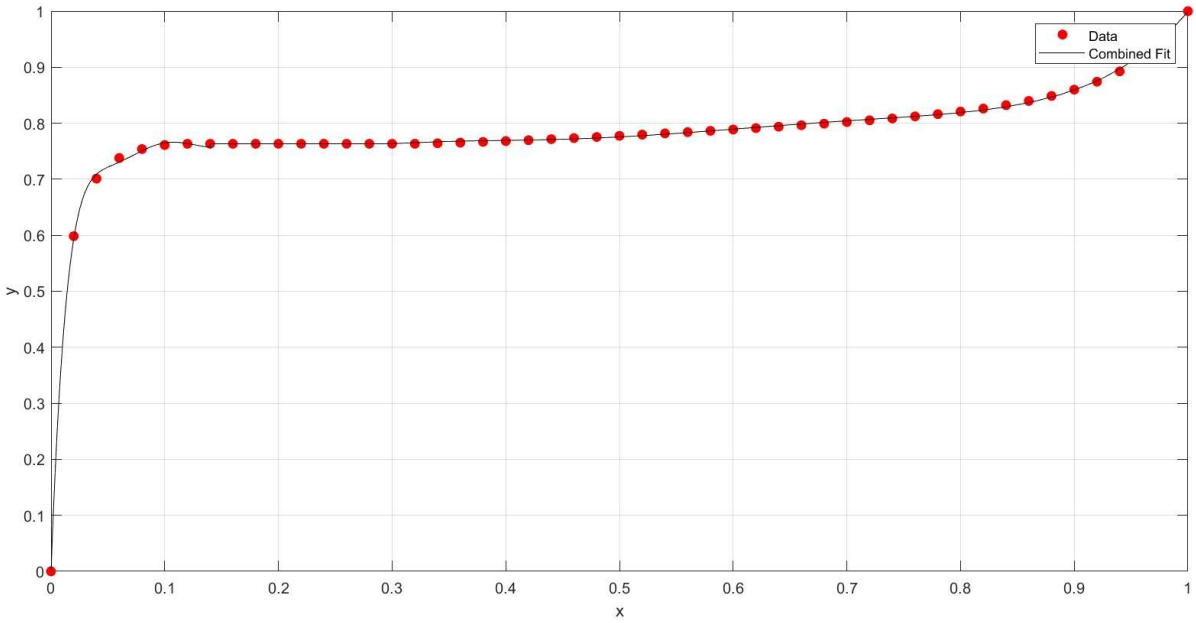

Figure A.1.2 Model for vapor liquid equilibria of the mixture, model and real data.

Code

```
clear all;
clc;
opengl('save', 'software');

% Feed, distillate, and bottom specifications
xd = 0.75;
xb = 0.0002;
zf = 0.03;
q = 0.97;  % Feed quality
F = 84.84;  % Feed flow rate in kmol/h

% Mole fractions
x_THF = 0.026;  % Mole fraction of THF
x_Water = 0.974;  % Mole fraction of Water
```

```
q_target = q;  % Desired q value (You can change this to test different q values)

%% LATENT HEAT OF VAPORIZATION
H_vap_THF = 29563.9;  % THF latent heat of vaporization at 1 atm (J/mol)
H_vap_Water = 40660;  % Water latent heat of vaporization at 1 atm (J/mol)

%% SPECIFIC HEAT FUNCTIONS FOR THF
% Cp functions for THF (Liquid and Vapor)
Cp_THF_L = @(T) 0.2260.*T + 116.2337;  % J/mol°C (Liquid)
Cp_THF_V = @(T) 0.2261.*T + 105.3780;  % J/mol°C (Vapor)

%% SPECIFIC HEAT FUNCTIONS FOR WATER
% Cp function for Water (Liquid and Vapor)
Cp_WATER_L = @(T) 0.0009.*T.^2 - 0.0514.*T + 76.107;  % J/mol°C (Liquid)
Cp_WATER_V = @(T) 0.0001.*T.^2 + 0.0103.*T + 103.2527;  % J/mol°C (Vapor)

%% ENTHALPY FUNCTIONS FOR THF AND WATER
% Define the enthalpy of the liquid and vapor as functions of temperature
H_L_THF = @(T) Cp_THF_L(T) * (T - 25);  % Reference temperature of 25°C
H_V_THF = @(T) H_vap_THF + Cp_THF_V(T) * (T - 25);

H_L_Water = @(T) Cp_WATER_L(T) * (T - 25);  % Reference temperature of 25°C
H_V_Water = @(T) H_vap_Water + Cp_WATER_V(T) * (T - 25);

% Enthalpy of the feed (assuming 50% vapor and 50% liquid as an example)
H_F_THF = @(T) 0.5 * (H_L_THF(T) + H_V_THF(T));  % Example as a mixture
H_F_Water = @(T) 0.5 * (H_L_Water(T) + H_V_Water(T));  % Example as a mixture

% Total enthalpy functions for the mixture
H_L = @(T) x_THF * H_L_THF(T) + x_Water * H_L_Water(T);  % Total liquid enthalpy
H_V = @(T) x_THF * H_V_THF(T) + x_Water * H_V_Water(T);  % Total vapor enthalpy
H_F = @(T) x_THF * H_F_THF(T) + x_Water * H_F_Water(T);  % Total feed enthalpy

% Define the function for q
q_fun = @(T) (H_L(T) - H_F(T)) / (H_L(T) - H_V(T)) - q_target;

% Check the function values at the endpoints of the interval
q_at_0 = q_fun(0);
q_at_150 = q_fun(150);

%fprintf('q(0°C): %f\n', q_at_0);
%fprintf('q(150°C): %f\n', q_at_150);

% Check if the signs are the same
if sign(q_at_0) == sign(q_at_150)
    % If the signs are the same, use fminbnd to minimize the difference
    %fprintf('Using fminbnd as a fallback...\n');
    T_solution = fminbnd(@(T) abs(q_fun(T)), 0, 150);  % Minimize the absolute difference
```

```
else
    % If the signs are different, use fzero
    T_solution = fzero(q_fun, [0, 150]);  % Search for a solution between 0°C and 150°C
end

fprintf('The temperature of the mixture for q = %4.2f is: %4.2f°C\n', q_target, T_solution);



% Equilibrium curve
% Fitting data
y1 = @(x) 4.8851e+06.*x.^7 - 4.2504e+06.*x.^6 + 1.5078e+06.*x.^5 - 2.8073e+05.*x.^4 + 2.9444e+04.*x.^3 - 1.7393e+03.*x.^2 + 54.7078.*x;
y2 = @(x) -2.3933e-15.*x + 0.7633;
y3 = @(x) 17.5661.*x.^5 - 50.3215.*x.^4 + 56.0001.*x.^3 - 30.0252.*x.^2 + 7.8025.*x - 0.0233;
y_eq = @(x) (x>=0 & x<=0.14).*y1(x) + (x>0.14 & x<=0.3).*y2(x) + (x>0.3 & x<=1).*y3(x);

% Plot the equilibrium curve
figure;
h1 = fplot(y_eq, [0 1], 'r', 'LineWidth', 2); hold on;
h2 = plot([0 1], [0 1], '--k');

% Feed line
feed = @(xq) q*xq/(q-1) - zf/(q-1);

% Plot the feed line within the range of the equilibrium curve
h3 = fplot(@(xq) min(feed(xq), y_eq(xq)), [0, 1], '--b');  % Ensure it doesn't exceed the equilibrium curve

% Find pinch point (intersection of feed line and equilibrium curve)
x_pinch = fsolve(@(xq) feed(xq) - y_eq(xq), zf, optimset('Display','off'));
y_pinch = feed(x_pinch);

% Minimum reflux ratio
Rmin = (xd - y_pinch) / (xd - x_pinch) / (1 - (xd - y_pinch) / (xd - x_pinch));

% Print the minimum reflux ratio
fprintf('Minimum reflux ratio: %4.2f\n', Rmin);

% Actual reflux ratio
R = 1.5 * Rmin;
% Print the actual reflux ratio
fprintf('Actual reflux ratio: %4.2f\n', R);

% Calculate the distillate flow rate D using the feed flow rate F
D = F * (R + 1) * zf / ((R + 1) * xd - xb);
```

```
% Print the distillate flow rate
fprintf('Distillate flow rate: %4.2f kmol/h\n', D);

% Calculate the bottoms flow rate B using the results
B = F - D;

fprintf('Bottoms flow rate: %4.2f kmol/h\n', B);

% Calculate Light Key Recovery
LK_recovery = (F * zf - B * xb )*100/ (F * zf);

% Display the result
fprintf('The Light Key Recovery is: %4.2f%%\n', LK_recovery);

% Calculate Heavy Key Recovery
HK_recovery = (( D * (1 - xd)) / (F * (1-zf))) * 100;

% Display the result
fprintf('The Heavy Key Recovery is: %4.2f%%\n', HK_recovery);


% Rectifying line (at R = 1.5*Rmin)
OpRect = @(xq) R/(R+1)*xq + xd/(R+1);

% Find intersection of rectifying line and feed line
x_inters = fsolve(@(xq) OpRect(xq) - feed(xq), x_pinch, optimset('Display','off'));
y_inters = OpRect(x_inters);

% Stripping line
OpStrp = @(xq) y_inters + (xq - x_inters) * (xb - y_inters) / (xb - x_inters);

% Plot feed, rectifying, and stripping lines
h4 = fplot(OpRect, [x_inters, xd], '-g', 'LineWidth', 2);
h5 = fplot(OpStrp, [xb, x_inters], '-m', 'LineWidth', 2);
plot([0 1], [0 1], '--k');  % 45-degree line

% Stepping off stages (Rectifying Section)
xr(1) = xd;
yr(1) = xd;
i = 1;
while xr(i) > x_inters
    xr(i+1) = fsolve(@(xq) y_eq(xq) - yr(i), xr(i), optimset('Display','off'));
    yr(i+1) = OpRect(xr(i+1));
    plot([xr(i) xr(i+1)], [yr(i) yr(i)], 'k-o');  % Horizontal step
    plot([xr(i+1) xr(i+1)], [yr(i) yr(i+1)], 'k-o');  % Vertical step

    % Add stage number
```

```
    text((xr(i) + xr(i+1)) / 2, yr(i), num2str(i), 'VerticalAlignment', 'bottom', 'HorizontalAlignment', 'right');

    i = i + 1;
end
ir = i - 1;

% Stepping off stages (Stripping Section)
xs(1) = xr(end);
ys(1) = yr(end);
j = 1;
while xs(j) > xb
    xs(j+1) = fsolve(@(xq) y_eq(xq) - ys(j), xs(j), optimset('Display','off'));
    ys(j+1) = OpStrp(xs(j+1));
    plot([xs(j) xs(j+1)], [ys(j) ys(j)], 'k-o');  % Horizontal step
    plot([xs(j+1) xs(j+1)], [ys(j) ys(j+1)], 'k-o');  % Vertical step

    % Add stage number
    text((xs(j) + xs(j+1)) / 2, ys(j), num2str(ir + j), 'VerticalAlignment', 'top', 'HorizontalAlignment', 'right');

    j = j + 1;
end
js = j - 1;

% Add legend
legend([h1 h3 h4 h5], {'Equilibrium Curve', 'Feed Line', 'Rectifying Line', 'Stripping Line'}, 'Location', 'Best');

xlabel('Liquid Mole Fraction (x)');
ylabel('Vapor Mole Fraction (y)');
title('McCabe-Thiele Diagram');
grid on;

% Set axis limits to display only between 0 and 1
axis([0 1 0 1]);

% Number of stages
N_total = ir + js;
fprintf('Total number of stages: %d\n', N_total);
fprintf('Optimal feed stage location: %d\n', ir);

% Given overall efficiency
efficiency = 0.6;

% Theoretical number of stages (calculated from McCabe-Thiele)
N_theoretical = ir + js;  % ir is for rectifying section, js for stripping
```

```
% Actual number of stages
N_actual = ceil(N_theoretical / efficiency);

% Print the actual number of stages
fprintf('Actual number of stages: %d\n', N_actual);
```

A.2. SAFETY MANAGEMENT OF PEROXIDE-FORMING CHEMICALS: TETRAHYDROFURAN (THF)

Peroxide Formation in Tetrahydrofuran (THF)[4]

Peroxides are reactive chemical species characterized by the presence of an oxygen-oxygen single bond (–O–O–). Organic peroxides typically conform to the structures R–O–O–R or R–O–O–H, where *R* denotes an organic group. These compounds are of particular concern in laboratory and industrial environments due to their high instability and potential for explosive decomposition.

- **Hazards Associated with Organic Peroxides**
- **Explosive Decomposition:** Peroxides can detonate upon exposure to heat, friction, impact, or during processes such as evaporation or distillation, particularly when concentrated.
- **Radical Reactivity:** The weak O–O bond easily dissociates to form free radicals, which can propagate chain reactions and escalate into uncontrolled, exothermic events.
- **Environmental Sensitivity:** Peroxides are susceptible to light and elevated temperatures, both of which accelerate their degradation and increase the risk of violent decomposition.
- **Undetectable Accumulation:** Peroxide formation is often not visually apparent. Ethers like THF can appear stable while harboring dangerous peroxide levels, making the risk of accidental detonation higher.
- **Toxicological Risks:** In addition to physical hazards, some peroxides and their decomposition products are toxic, posing health risks through inhalation or dermal exposure.
- **Mechanism of Peroxide Formation in THF**

THF is highly prone to autoxidation in the presence of air and light, forming hazardous peroxide species over time.

1. **Initiation – Autoxidation:** Light, heat, or trace metal impurities can abstract a hydrogen atom from the methylene group adjacent to the oxygen in the ether ring, forming a carbon-centered radical.
2. **Radical Reaction with Oxygen:** The alkyl radical rapidly reacts with atmospheric O_2 to form a peroxyl radical.
3. **Propagation:** The peroxyl radical abstracts hydrogen from another THF molecule, forming a hydroperoxide (THF–OOH) and propagating the radical chain.
4. **Termination:** Radicals may recombine to form stable products, but in the absence of decomposing agents or inhibitors, hydroperoxides can accumulate over time.

- **Peroxide-Forming Chemical Classification**

Peroxide-forming chemicals (PFCs) are categorized based on the nature and severity of their hazard:

Category	Hazard Nature	Description
A	High hazard without concentration	Form peroxides that may detonate without concentration. Insoluble peroxides accumulate near container threads. E.g., Isopropyl ether.

[4] Tucker, J. W., & Davidson, J. P. (2015). *Development of improved peroxide formation procedures for laboratory chemicals*. Organic & Biomolecular Chemistry, 13(12), 3349–3353. https://doi.org/10.1039/C5OB00012B

B	Hazard upon concentration	Peroxides concentrate as solvent evaporates, especially dangerous during distillation. E.g., Tetrahydrofuran (THF).
C	Explosive polymerization hazard	Peroxides can trigger violent polymerization. Common in vinyl monomers like styrene, methyl acrylate, or vinyl ethers.

THF is classified as a **Category B** PFC due to its tendency to form explosive peroxides upon concentration.

Safe Handling and Storage of THF[5]

To mitigate risks associated with THF and other PFCs, strict safety protocols must be implemented:

- **Storage Guidelines**
- **Cool, Dark Conditions:** Store THF away from light and heat to minimize autoxidation.
- **Properly Sealed Containers:** Oxygen can permeate imperfect seals. Ensure caps are tightened adequately—neither too loose (to prevent peroxide buildup around threads) nor overly tight (to avoid uneven sealing).
- **Contamination Control:** Keep containers free from dust and metal particles that may catalyze peroxide formation.
- **Use of Inhibitors:** Purchase THF with added peroxide inhibitors (e.g., BHT). If using uninhibited THF, store under inert gas (nitrogen or argon) to suppress peroxide formation. Note: Inhibitors for **Category C** substances often require oxygen and are not suited for inert storage.

Labeling and Inspection Requirements

Each container of THF or other PFCs should be clearly labeled with:

- Date of receipt
- Date of opening
- Expiry date
- Presence/type of inhibitor
- Date and results of last peroxide test (if applicable)
- **Warning Signs of Peroxide Formation**
- White crystalline deposits around the cap or inside the container
- Oily layers, precipitates, or increased viscosity
- Crust formation or discoloration (in solids)
- Residue after evaporation

Containers beyond their shelf life or showing signs of degradation should be handled with extreme caution.

[5] University of Wisconsin–Madison Environment, Health & Safety. (2020, August). *Peroxide-forming chemicals: Safe storage and handling* (CHM-GUI-005). https://ehs.wisc.edu/wp-content/uploads/sites/1408/2020/08/CHM-GUI-005-NEW.pdf

Distillation Safety Measures

Distillation poses a major risk for PFCs due to potential peroxide concentration in the still pot. Though increasingly replaced by safer alternatives (e.g., column purification), distillation may still be necessary in some settings.

Critical Safety Practices:

- **Pre-Distillation Testing:** Always test for peroxides prior to distillation or evaporation.
- **Avoid Dry Distillation:** Never distill to dryness; retain at least 20% of the initial volume to avoid peroxide detonation.
- **Use of Diluting Agents:** Add mineral oil or other high-boiling solvents to reduce peroxide concentration in the still.
- **Reactive Metal Drying:** Sodium metal is sometimes used to both dry and reduce peroxides in ethers like THF. Use with caution—sodium reacts violently with water. Incorporate benzophenone as an indicator (deep blue color signals active sodium). Add sodium incrementally, and replenish when the blue color fades.

Conclusion

Tetrahydrofuran is a valuable solvent with significant peroxide-forming potential, particularly under improper storage or prolonged exposure to air and light. A clear understanding of the mechanisms, classification, and mitigation measures is essential to ensure its safe use. Through rigorous storage practices, regular monitoring, and adherence to appropriate handling protocols, the risks associated with THF can be effectively minimized in both laboratory and industrial environments.

A.3. CONFIDENTIAL ANNEX

Confidential information

Confidential information

Confidential information

A.4. COLUMN INTERNALS

Confidential information

Confidential information

A.5. COLUMN DESIGN

Confidential information

A.6. EXCHANGERS DESIGN

Confidential information

A.7. SAFETY DATA SHEETS

Confidential information